mosaic eyes: a zebrafish gene required in pigmented epithelium for apical localization of retinal cell division and lamination

Abbie M. Jensen*, Charline Walker and Monte Westerfield

Institute of Neuroscience, University of Oregon, Eugene, OR 97403-1254, USA

*Author for correspondence (e-mail: ajensen@uoneuro.uoregon.edu)

SUMMARY

For proper function of the retina, the correct proportions of retinal cell types must be generated, they must be organized into cell-specific laminae, and appropriate synaptic connections must be made. To understand the genetic regulation of retinal development, we have analyzed mutations in the *mosaic eyes* gene that disrupt retinal lamination, the localization of retinal cell divisions to the retinal pigmented epithelial surface and retinal pigmented epithelial development. Although retinal organization is severely disrupted in *mosaic eyes* mutants, surprisingly, retinal cell differentiation occurs. The positions of dividing cells and neurons in the brain appear normal in *mosaic eyes* mutants, suggesting that wild-type *mosaic eyes* function is specifically required for normal retinal development. We demonstrate that *mosaic eyes* function is required within the retinal pigmented epithelium, rather than in dividing retinal cells. This analysis reveals an interaction between the retinal pigmented epithelium and the retina that is required for retinal patterning. We suggest that wild-type *mosaic eyes* function is required for the retinal pigmented epithelium to signal properly to the retina.

Key words: Cell fate determination, *Danio rerio*, Eye, Mutation, Polarity, Proliferation, RPE

INTRODUCTION

Two major questions in developmental biology are how do cells become different from each other and how are different cell types organized into functional tissues or organs. Analysis of mutant mice has identified many genes that control the organization of cells into layers in the brain (for review, see Rice and Curran, 1999). Generally, these mutations do not affect neurogenesis, suggesting that cell positioning is largely independent from cell-fate determination. As yet, no targeted mutations in mammals have been reported to cause prominent lamination defects in the retina, suggesting that the neural retina, given its unique relationship with adjacent tissues, the lens and retinal pigmented epithelium (RPE), uses fundamentally different processes to generate cell layers than those used for brain lamination. Recently, several mutations in zebrafish have been isolated that cause retinal lamination defects (Malicki et al., 1996; Malicki and Driever, 1999) and all of these mutations have accompanying RPE defects, suggesting that the RPE may be required for normal retinal lamination. Alternatively, the genes that regulate the positioning of retinal cells may also function in the development of the RPE. Evidence from in vitro and in vivo experiments suggests that the RPE is required for normal retinal organization (Vollmer et al., 1984; Rothermael et al., 1997; Raymond and Jackson, 1995). Vollmer and colleagues (Vollmer et al., 1984) demonstrated that the inclusion of RPE cells in retinal reaggregate cultures could induce a highly organized arrangement of cells that was similar to that observed in vivo. Rothermel and colleagues (Rothermel et al., 1997) further demonstrated that RPE-conditioned media could have a similar affect on retinal reaggregates, suggesting that the RPE factor or factors is diffusible. In vivo experiments by Raymond and Jackson (Raymond and Jackson 1995), in which they genetically ablated RPE cells using diphtheria toxin, demonstrated that the development of layers in the retina was severely perturbed in the absence of RPE. Although these experiments suggest that the RPE has an important role in retinal organization, the mechanisms by which the RPE signals to the retina and the genes that regulate this process are not yet known.

We have isolated two mutations of the *mosaic eyes* (*moe*) gene in which there are RPE defects, a loss of lamination in the retina, a loss of localization of dividing retinal cells to the RPE surface, but no apparent disorganization of cells in the brain. Although the retina is severely disorganized, retinal cells differentiate in *moe* mutant retinas. The localization of dividing *moe* mutant retinal cells transplanted into wild-type hosts is normal, suggesting that the *moe* mutation does not act cell autonomously in retinal cells. We show that *moe* function is required in the RPE: transplanted wild-type RPE cells can rescue the mislocalization of dividing cells in *moe* mutant retinas. Our analysis provides the first genetic evidence that signaling from the RPE to the retina is required for the induction of proper retinal organization. We suggest that this signaling depends upon *moe* gene function.

MATERIALS AND METHODS

Fish

We identified *moe*[b476] in a screen for abnormal eye morphology of 2-day-old haploid embryos produced by the F1 progeny of fish generated by in vitro fertilization of *AB strain eggs with γ-irradiated *AB strain sperm (Walker, 1999). To find additional alleles of *moe*, we crossed *moe*[b476]/+ females with males carrying mutations induced by *N*-ethyl-*N*-nitrosourea (ENU; Riley and Grunwald, 1995). We examined the progeny from 327 males crossed to *moe*[b476]/+ females for phenotypes present in *moe*[b476]/*moe*[b476] embryos. We found one male that when crossed with *moe*[b476]/+ females produced embryos that appeared identical to *moe*[b476]/*moe*[b476] embryos, thus representing non-complementation of the *moe* locus. This allele is termed *moe*[b781]. Embryos were maintained at 28.5°C and developmental stages are given as hours postfertilization (h) or days postfertilization (d).

In situ hybridization

Frozen sections

Embryos were fixed in 4% paraformaldehyde in PBS overnight at 4°C, washed with PBS, embedded in 1.5% agar with 5% sucrose, and equilibrated in 30% sucrose in PBS. Cryostat sections (16 μm) were cut and transferred onto slides coated with Vectabond (Vector laboratories), air dried for 1-6 hours at room temperature and used immediately or stored desiccated at –20°C.

Probe preparation

cDNA templates (opsin cDNAs were gifts from J. Dowling, apoe cDNA was a gift from B. Thisse and C. Thisse) were used to generate digoxigenin (DIG)-labeled antisense RNA probes: rhodopsin linearized with *Xba*I, transcribed with T7 polymerase; blue opsin linearized with *Xba*I, transcribed with T7 polymerase; red opsin linearized with *Sac*I, transcribed with T7 polymerase. Preparation of RNA probes with DIG-UTP was performed according to the manufacturer's recommendations (Boehringer Mannheim). Briefly, 1 μg of linearized template was transcribed in a total volume of 20 μl using T7 polymerase (Boehringer Mannheim) and DIG-UTP (Boehringer Mannheim) for 2 hours at 37°C. The reaction products were precipitated, resuspended in 100 μl water or hybridization buffer, and stored at −20°C. DIG-labeled RNA probes (dct probe, gift from R. Kelsh) were diluted in hybridization buffer (50% formamide, 10% dextran sulfate, 1 mg/ml yeast RNA, 1× Denhardt's and 1× salt) and denatured for 10 minutes at 70°C.

Hybridization

Approximately 100 μl of diluted probe was placed on the sections and a coverslip placed on top. Sections were hybridized overnight at 65°C in a humidified box. The slides were washed twice in 50% formamide, 1× SSC, 0.1% Tween-20 (Tw) at 65°C for 30 minutes followed by two washes in MABT (100 mM maleic acid, 150 mM NaCl, pH 7.5, 0.1% Tw) for 30 minutes at room temperature. Sections were blocked for 2-4 hours at room temperature in MABT containing 20% sheep serum (Sigma) and 2% blocking reagent (Boehringer Mannheim). The blocking solution was then replaced with blocking solution containing a 1:3000 dilution of alkaline-phosphatase-conjugated Fab fragments of sheep anti-DIG antibodies (Boehringer Mannheim), a coverslip placed over the antibody solution, and the slides were incubated overnight at 4°C in a humidified box. The slides were washed a minimum of five times in MABT for 20 minutes at room temperature, washed twice in staining buffer (100 mM NaCl, 50mM MgCl₂, 100 mM Tris pH 9.5 and 0.1% Tw) and incubated in the dark at room temperature overnight in staining buffer plus 10% v/vw polyvinyl alcohol (MW 70,000-100,000; Sigma) containing 4.5 μl NBT and 3.5 μl BCIP/ml (Boehringer Mannheim). The slides were washed in distilled water, dehydrated to 100% ethanol, cleared with xylene and mounted in DPX (Fluka).

Histology

Frozen sections (16 μm) or thin plastic sections (3 μm) were incubated in 0.05% thionin in 0.1 M acetate for 5 minutes, dehydrated through a series of increasing ethanol concentrations, washed in xylene, and mounted in DPX (Fluka).

Immunohistochemistry

Sections were prepared as described above. Sections were rehydrated in PBS, incubated in blocking solution (20% goat serum in 50 mM Tris buffer (pH 7.4), 10 mM lysine, 145 mM NaCl, 1% BSA, and 0.1% Tween) for 30 minutes, incubated overnight at 4°C in primary antibody diluted in blocking solution: rabbit anti-GABA, 1:1000 (Sigma); rabbit anti-carbonic anhydrase II, 1:1000 (gift from P. Linser); mouse Zn5 supernatant, 1:50 (Trevarrow, 1990); rabbit anti-phospho-histone H3, 1:1000 (Upstate Biotechnology); mouse anti-HU, 1:100 (monoclonal 16A11 ascites; Marusich, 1993); rabbit anti-CRABP, 1:1000 (gift from J. Saari); mouse Zpr1 and Zpr3, 1:200 (University of Oregon Monoclonal Facility). The sections were washed multiple times in PBS plus 0.1% Tween (PBS-Tw), and then incubated in fluorescein- or rhodamine-conjugated secondary antibodies: goat anti-mouse immunoglobulin IgG+IgM, 1:100 (Jackson ImmunoChemicals) or Alexis Ig, 1:200 (Molecular Probes) or goat anti-rabbit, 1:200 (Alexis, Molecular Probes) diluted in blocking solution plus 0.1% Tw. After washing in PBS-Tw, the coverslips were mounted onto the glass slides in 50% glycerol:50% Tris (pH 8.3) or Vectashield (Vector Laboratories) and examined with a Zeiss Axioskop or Zeiss Axioplan fluorescence microscope.

Bromodeoxyuridine labeling

To birthdate retinal ganglion cells, we incubated wild-type and *moe* mutant embryos in 10 mM bromodeoxyuridine (BrdU) in embryo medium from 42 h to 60 h, at which time we fixed the embryos in 4% paraformaldehyde. To birthdate photoreceptors, we incubated wild-type and *moe* mutant embryos in 10 mM BrdU in embryo medium from 50 h to 74 h, then allowed the embryos to develop in BrdU-free embryo medium until we fixed the embryos at 4 d in 4% paraformaldehyde. Frozen sections were labeled with Zn5, or Zpr1+Zpr3 as described above. Then we incubated the sections with the following solutions: in 4% paraformaldehyde, washed in PBS-Tw, cold acid:alcohol (5:95) for 10 minutes, washed, 2 M HCl for 30 minutes, washed, 0.1 M sodium borate (pH 8.5) for 30 minutes, washed, blocking solution for 30 minutes, rat anti-BrdU supernatant (neat; Accurate Chemicals) for 4 hours, washed, donkey fluorescein-anti-rat (1:100; Jackson ImmunoChemicals), and washed. Sections were mounted in 50% glycerol:50% Tris (pH 8.3). Confocal images (approximately 1 μm optical thickness) were acquired using a Zeiss 310 Laser Scanning Microscope and 63× Neofluar objective using the overlay function.

Blastomere transplantations

Retinal mosaics

Embryos used for transplantation experiments were produced by intercrossing *moe*[b476]/+ fish, thus, yielding a wild-type to mutant embryo ratio of 3:1. To label donor embryos, a mixture of 3% rhodamine-dextran (Molecular Probes, D3308) and 3% biotin-dextran (Molecular Probes, D7135) in 0.2 M KCl was pressure-injected into the yolk of two- to four-cell stage embryos. We used transplantation methods similar to those previously described (Ho and Kane, 1990). At the high stage to dome stage, approximately 20-40 cells were transplanted from labeled-donor embryos into one or two unlabeled-host embryos. To inhibit pigmentation, 0.003% 1-phenyl-2-thiourea (Sigma) was added to the embryo medium at 20-24 h. The assignment of host and donor genotypes (wild type versus mutant) was assessed by morphological phenotypic criteria at 30-48 h and reconfirmed upon labeling with anti-H3 antibodies. For anti-H3 antibody labeling, donor

and host embryos were fixed at 36 h or 48 h in 4% paraformaldehyde in PBS overnight at 4°C, processed and sectioned as described above for immunocytochemistry with anti-H3 antibody. Confocal images (approximately 2.3 µm optical thickness) were acquired using a Zeiss 310 Laser Scanning Microscope and 40× Neofluar (0.75 numerical aperture) objective. For photoreceptor labeling (Zpr1 and Zpr3 antibody), embryos were fixed at 4 d. Confocal images (approximately 1 µm optical thickness) were acquired using a Zeiss 310 Laser Scanning Microscope and 63× Neofluar objective.

RPE mosaics

The methods for generating RPE mosaics are similar to those used for generating retinal mosaics with the following modifications. We transplanted large numbers (50-100) of labeled blastomeres from wild-type embryos (produced from wild-type intercrosses) into embryos produced by intercrossing *moe*[b476]/+ fish. Embryos were fixed at approximately 42 h and processed for immunocytochemisty with anti-H3 as described above. Photos were taken using a Zeiss Axioplan microscope and the two color channels (red, lineage tracer and green, anti-H3) were overlaid using the screen function in Adobe Photoshop.

Genetic mapping

moe[b476]/AB fish were crossed to WIK/WIK strain fish. We used haploid and parthenogenetic diploid (Streisinger et al., 1981) embryos for genetic mapping. We isolated genomic DNA from individual phenotypically wild-type and mutant 2 d embryos. The ratio of wild-type to mutant embryos (228:182) in parthenogenetic diploid clutches allowed us to estimate the genetic distance between the *moe* locus and the centromere. We performed PCR analysis with SSLP (Johnson et al., 1996) markers close to the centromere of each linkage group using DNA from eight pooled individual wild-type embryos and eight pooled mutant embryos and found tight cosegregation of the *moe* mutant phenotype with centromeric SSLP markers on LG9. We then refined the map by testing additional SSLP markers that are centromeric on LG9 using DNA from individual wild-type and mutant embryos. The genetic distance of the *moe* locus from each SSLP marker is based on the number of recombinations in more than 150 individual meiotic events. LOD scores were calculated using Map Manager software.

RESULTS

The *moe* mutation disrupts retinal and RPE patterning

We isolated two *moe* alleles, *moe*[b476] and *moe*[b781], that are phenotypically indistinguishable. Our analysis is based primarily on the *moe*[b476] allele. The *moe* mutation is recessive lethal (homozygous embryos die around 6 d), inherited in a Mendelian fashion and produces several prominent phenotypes. At 36 h, *moe* mutants exhibited an enlarged heart cavity and abnormal heart morphology, dorsal curvature of the tail and reduced brain ventricles (Fig. 1B). At 2 d, a circulation and heart defect was apparent in *moe* mutants. The RPE was also abnormal in *moe* mutants. At 2 d, the RPE in wild-type eyes formed a continuous sheet (Fig. 1C), whereas in *moe* mutant eyes, the RPE appeared patchy (Fig. 1D). Histological examination of internal eye structure, revealed that lamination was severely disrupted in *moe* mutants. At 3 d, the three nuclear layers (retinal ganglion cell, inner nuclear and outer nuclear) were well delineated in histological sections of wild-type retinas (Fig. 1E); in *moe* mutant retinas, the nuclear layers were absent (Fig. 1F).

The *moe* mutant is distinct from other retinal patterning mutants

To learn whether *moe* might be allelic to other zebrafish mutations that affect retinal organization, we mapped the *moe* locus by co-segregation with simple sequence length polymorphisms (SSLPs). By measuring the percentage of *moe* mutant embryos in clutches of parthenogenetic diploid embryos, we obtained the recombination frequency and calculated the genetic distance from the *moe* locus to the centromere, which is approximately 5.6 centiMorgans (cM). By scoring SSLP markers that co-segregated with the *moe* locus, we mapped the *moe* locus to the centromeric region of LG9. The closest SSLP markers are z6430 (1.5-2 cM distal, towards the telomere, minimum LOD is 28) and z13213 (1-1.5 cM proximal, towards the centromere, minimum LOD is 51). These results show that *moe* is not an allele of the previously described *oko meduzy* and *nagie oko* mutations because these two loci are on different chromosomes (J. Malicki, personal communication). Furthermore, *moe* is not allelic to *heart and soul*, as indicated by genetic complementation analysis (data not shown). Taken together, this analysis suggests that the *moe* mutations identify a novel locus involved in retinal development.

Retinal cell types differentiate in *moe* mutants

To determine whether cells differentiate in the disorganized retina of *moe* mutants, we used cell-specific antibodies and RNA probes to assess the development of various cell types. All cell types we examined, including retinal ganglion cells, amacrine cells, Müller glial cells and photoreceptors, formed in *moe* mutant retinas. Although these cells differentiated, they were in abnormal positions (Fig. 2). Retinal ganglion cells, recognized by the anti-DM GRASP antibody, Zn5 (Trevarrow et al., 1990; Fashena and Westerfield, 1999) are the first cells to differentiate in the zebrafish retina (L. W. Nawrocki, PhD thesis, University of Oregon, 1985). In wild-type retinas, retinal ganglion cells formed the cell layer that is closest to the lens (Fig. 2A). In *moe* mutant retinas, many ganglion cells were in abnormal positions, even adjacent to the RPE (Fig. 2B, arrowheads). Although many retinal ganglion cells were in ectopic locations, an optic nerve formed in *moe* mutant retinas (Fig. 2B, arrow). Amacrine cells, recognized by mRNA in situ hybridization with apoe probe (Babin et al., 1997), normally lie in the inner nuclear layer (Fig. 2C). In *moe* mutant retinas, amacrine cells developed, but they were disorganized (Fig. 2D). We often observed a reduction in the numbers of apoe-positive cells (data not shown). We also labeled amacrine cells with anti-GABA (Sandell et al., 1994) and anti-CRABP antibodies (De Leeuw et al., 1990), and observed similar results to the apoe labeling (data not shown). Müller glial cells, recognized by anti-carbonic anhydrase II antibodies (Linser et al., 1985), normally lie in the middle of the inner nuclear layer and send radial processes to both the vitreal surface and the outer limiting membrane (Fig. 2E). In *moe* mutant retinas, Müller glial cells developed but their numbers appeared reduced, they were disorganized, and radial processes were absent (Fig. 2F). The reduction in amacrine cells and Müller glia in *moe* mutant retinas could be due to the increased cell death we observed at late stages of development (48 h and 60 h; data not shown). We examined the development of three types of photoreceptors, rods, red
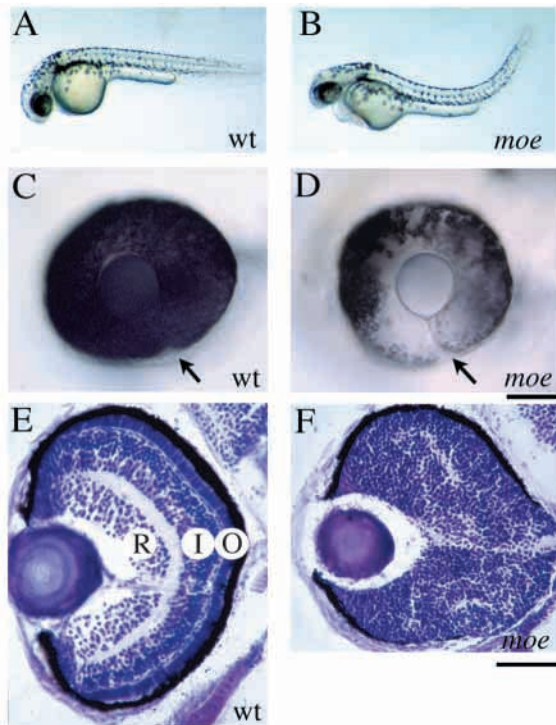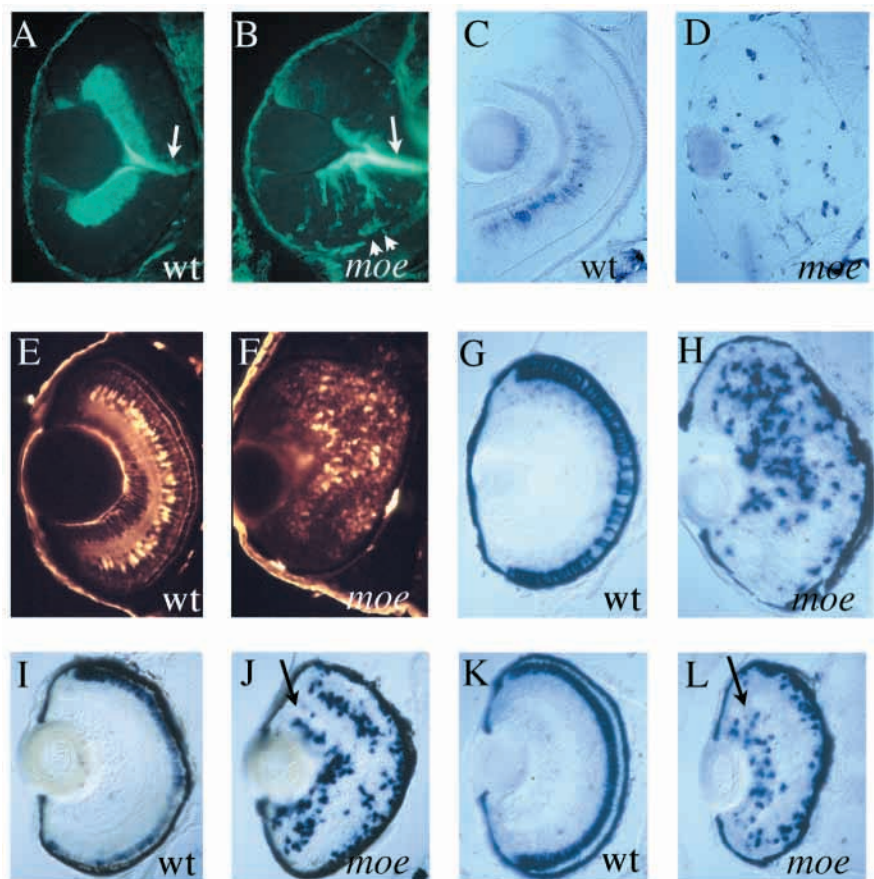
Fig. 1. The *moe* mutation affects the eye and body shape. Views of live (A) wild-type and (B) *moe* mutant embryos at 36 h. *moe* mutants have reduced brain ventricle volume, heart cavity swelling, distended heart, dorsal curvature of the tail and reduced eye pigmentation. Higher magnification views of live wild-type (C) and *moe* mutant (D) eyes at 2 d. The RPE is uniform in wild-type eyes (C) but is patchy in *moe* mutant eyes (D). Arrows indicate the choroid fissure (C,D). Thionin-stained sections through wild-type (E) and *moe* mutant (F) retinas at 3 d. The three nuclear layers, retinal ganglion cell layer (R), inner nuclear layer (I) and outer nuclear layer (O) are visible in wild-type retinas (E). Retinal organization is severely disrupted in *moe* mutant retinas (F) and no definable layers are apparent. Scale bars: 50 μm.

cones and blue cones, by mRNA in situ hybridization with photoreceptor-specific opsin probes (Robinson et al., 1995). Normally, photoreceptors lie adjacent to the RPE (Fig. 2G,I,K). In *moe* mutant retinas, photoreceptors formed but they were in abnormal positions (Fig. 2H,J,L). In some *moe* mutants, cryptic or partial photoreceptor layers formed in the inner parts of the retina, and in some cases ectopic photoreceptor layers formed in the position normally occupied by retinal ganglion cells (Fig. 2J,L, arrows). None of the differentiated cell types that we examined formed rosettes as previously observed in retinas in which the RPE was ablated (Raymond and Jackson, 1995).

Fig. 2. Retinal cell types differentiate in *moe* mutant retinas but are abnormally positioned. (A) Retinal ganglion cells, labeled with anti-DM-GRASP antibody (Zn5), lie in the retinal ganglion cell layer in wild-type retinas at 2 d. (B) Retinal ganglion cells differentiate in *moe* mutant retinas but many are in abnormal positions, scattered throughout the thickness of the epithelium, and some are adjacent to the RPE (arrowheads). The arrows indicate the optic nerve head, visible in both the wild-type (A) and *moe* mutant (B) retinas. Amacrine cells, labeled by in situ hybridization with apoe probe (C,D), lie in the inner nuclear layer in wild-type retinas at 4 d (C). Amacrine cells differentiate in *moe* mutant retinas but are in abnormal positions (D). Müller glial cells, labeled by anti-carbonic anhydrase antibodies (E,F), lie in the inner nuclear layer and send processes to both the vitreal and RPE surface in wild-type retinas at 4 d (E). Some Müller glial cells differentiate in *moe* mutant retinas, but they are scattered throughout the epithelium and their numbers appear reduced (F). Photoreceptors were identified using opsin specific gene probes at 5 d. Rod photoreceptors (G), labeled with rhodopsin probe, red cone photoreceptors (I), labeled with red opsin probe, and blue cone photoreceptors (K), labeled with blue opsin probe, lie in the outer nuclear layer, adjacent to the RPE in wild-type retinas. Rod (H), red cone (J) and blue cone (L) photoreceptors differentiate in *moe* mutant retinas but are in

abnormal positions and are often scattered throughout the epithelium. In some cases, cryptic photoreceptor layers form in ectopic positions, sometimes closest to the lens (J,L, arrow), the site normally occupied by retinal ganglion cells. Scale bar, 50 μm
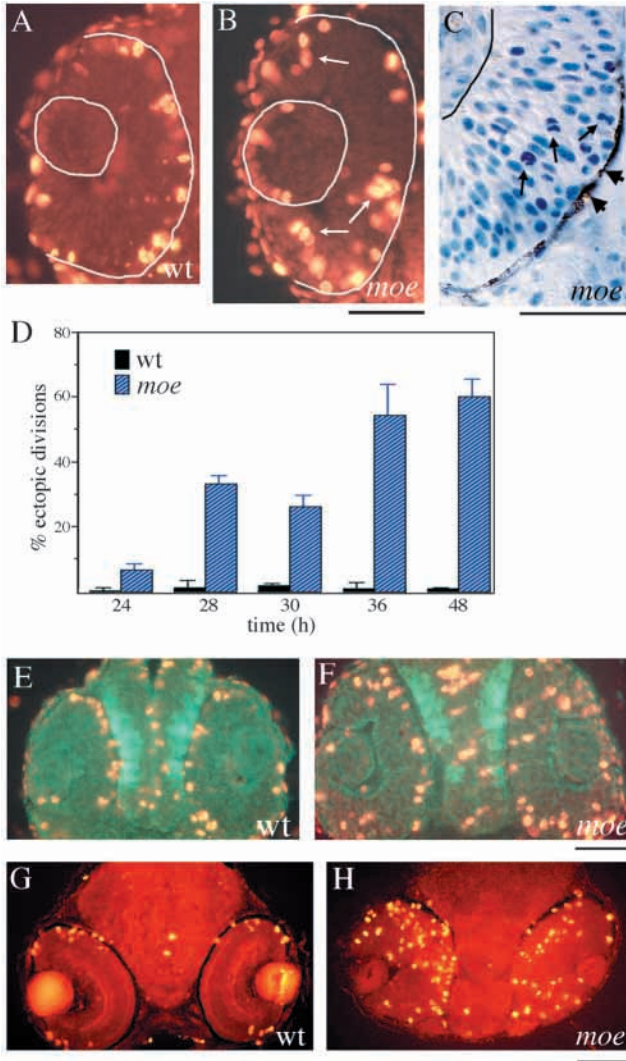
Fig. 4. Some retinal neuroepithelial cells have normal morphologies in *moe* mutants. We examined retinal neuroepithelial cell morphology at 36 h by transplanting blastomeres from rhodamine-labeled wild-type donor embryos into unlabeled wild-type host embryos, and transplanting blastomeres from rhodamine-labeled *moe* mutant donor embryos into unlabeled *moe* mutant host embryos. Rhodamine-labeled donor-derived cells are yellow. (A) Many labeled wild-type cells span the retinal neuroepithelium and extend processes to both the vitreal (basal) and RPE (apical) surfaces. (B) Many labeled *moe* mutant cells span the retinal neuroepithelium and extend processes to both the vitreal (basal) and RPE (apical) surfaces. Scale bar: 50 μm.

We examined the differentiation of the RPE by mRNA in situ hybridization with *dopachrome tautomerase* (*dct*) probes. Dct is an enzyme involved in an intermediate step of melanin synthesis (Pawelek et al., 1980; Aroca et al., 1990; Tsukamoto et al., 1992). It is one of the earliest molecular markers of RPE differentiation (Steel et al., 1992). We found patchy expression of *dct* in *moe* mutant eyes (data not shown), suggesting that some RPE cells remain undifferentiated or are absent.

Retinal precursor cells divide ectopically in *moe* mutants

Prior to cell differentiation, the developing neural retina is a pseudostratified epithelium in which retinal neuroepithelial precursor cells send processes to both the RPE (apical) and vitreal (basal) surfaces (Sidman, 1961). As cells proceed through the cell cycle, their nuclei migrate between the two surfaces; as cells enter M-phase with their nuclei at the RPE surface, they retract their basal process and divide. To determine whether the defect in the positions of differentiated cells in *moe* mutant retinas is related to a defect in precursor cell division, we examined the positions of mitotic cells. To recognize mitotic cells in M-phase, we used antibodies against phosphorylated histone H3, which specifically labels cells in M-phase (anti-H3; Hendzel et al., 1997). At 30 h, which is near the beginning of retinal cell differentiation (L. W. Nawrocki, PhD thesis, University of Oregon, 1985; Hu and Easter, 1999), mitotic cells, as defined by anti-H3 labeling, are at the RPE surface in wild-type retinas (Fig. 3A). In *moe* mutant retinas, many mitotic cells were in ectopic positions distant from the RPE (Fig. 3B, arrows). We also examined the positions of mitotic figures by histological staining of 33 h *moe* mutant retinas and observed proportions of ectopic mitotic profiles

Fig. 3. Cells divide ectopically and proliferation persists in *moe* mutant retinas. To localize cells in mitosis, we labeled sections with anti-phosphorylated H3 antibodies (anti-H3). The RPE surface (A,B) and the lens (A-C) are outlined. (A) In 30 h wild-type retinas, anti-H3 labeled epithelial cells are adjacent to the RPE. (B) In 30 h *moe* mutant retinas, many anti-H3 labeled cells are not adjacent to the RPE (arrows). (C) Histological staining of a section through a 33 h *moe* mutant retina shows that cells divide ectopically (arrows) in regions where RPE cells are present and pigmented (arrowheads). (D) We quantified the proportion (number of ectopic divisions divided by total number of divisions) of ectopically dividing cells at various developmental times in wild-type and *moe* mutant retinas using the anti-H3 antibody. We scored anti-H3 labeled cells as ectopic if they were more than one cell diameter away from the RPE at 24 h and 36 h, and more than two cell diameters away from the RPE at 48 h. We excluded from our analysis cells at the retinal margins. The bars represent the averages of at least three retinas from three individuals (±s.e.m.). (E,F) The positions of neurons (as labeled by anti-HU antibodies, green) and mitotic cells (anti-H3 labeled, orange) in wild-type (E) and *moe* mutant (F) brains at 36 h. (F) The positions of neurons and dividing cells are apparently normal in *moe* mutant brains. Cell division (as indicated by anti-H3 labeling; G,H) continues in *moe* mutant retinas. (G) In wild-type retinas at 64 h, cell division is confined to a few cells in the periphery. (H) Many cells continue to divide throughout the retina in 64 h *moe* mutant retinas. Scale bars: 50 μm in A-C,E,F; 100 μm in G,H.
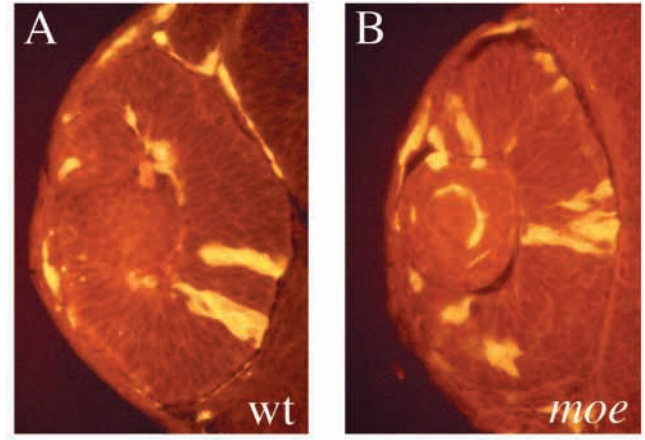
similar to those obtained by anti-H3 labeling (data not shown) and we observed ectopically dividing cells throughout the retina, not only in regions where the RPE layer lacks pigmentation (Fig. 3C).

To determine whether the proportions of ectopically dividing cells in *moe* mutant retinas change during development, we quantified the positions of mitotic cells in wild-type and *moe* mutant retinas at various times. At all time points examined, more cells divided ectopically in *moe* mutant retinas than in wild-type siblings (Fig. 3D). The proportion of ectopically dividing cells increased as development proceeded in *moe* mutant retinas, although the increase did not appear to be uniform with time; a large increase in ectopically dividing cells appeared between 24 h and 28 h, and another large increase appeared between 30 h and 36 h. We also determined that the numbers of dividing cells were not significantly different between wild-type and *moe* mutant retinas at early stages of development. We counted the number of dividing cells (H3$^+$) in a 180 μm strip that excluded the marginal zone in at least five sections/retina from three wild-type and three mutant embryos at 36 h. We found an average of 18.7±0.5 (s.e.m.) dividing cells/strip in wild-type retinas and 15.9±1.1 (s.e.m.) dividing cells/strip in *moe* mutant retinas. The values are not significantly different using student *t*-test analysis at $P<0.05$.

In contrast to the retina, the positions of neurons and dividing cells appeared normal in *moe* mutants in the midbrain (Fig. 3E,F), hindbrain and spinal cord (data not shown) as indicated by labeling with anti-H3 and with a pan neuronal antibody, anti-Hu (Marusich et al., 1993).

Not only do cells divide ectopically in *moe* mutant retinas, cells continue to divide after most division has ceased in wild-type retinas. By 64 h, cell division was confined to a small number of cells in the anterior margin in wild-type retinas (Fig. 3G). In contrast, large numbers of cells continued to divide throughout the retina in *moe* mutants (Fig. 3H).

Retinal epithelial cells can extend normal processes in *moe* mutants

To determine whether retinal cells divide in the wrong place in *moe* mutants because they are unable to form apical or basal attachments, we examined the morphology of retinal precursor cells in wild-type and *moe* mutant embryos. To label retinal precursor cells, we transplanted small groups of cells from blastula stage embryos labeled with rhodamine-dextran into unlabeled hosts of the same stage and then later examined the morphology of labeled donor cells that contributed to the retina. The embryos were the progeny of *moe^{b476}*/+ intercrosses, so that donors and hosts were either phenotypically wild type or mutant. We determined the genotypes after the embryos were phenotypically distinguishable. We examined the positions of labeled wild-type donor cells in wild-type hosts (Fig. 4A) and labeled *moe* mutant donor cells in *moe* mutant hosts (Fig. 4B) at 36 h. The morphology of labeled *moe* mutant cells suggested that *moe* mutant neuroepithelial cells can extend processes to both the RPE and vitreal surfaces (Fig. 4B). We also injected rhodamine-dextran into a single blastomere at the 16-cell stage, and then examined the morphology of labeled cells in wild-type and *moe* mutant retinas at 33 h, and again we observed retinal precursor cells extending apical and basal processes (data not shown). Thus, is seems unlikely that an inability to extend

apical and basal processes is the primary defect in *moe* mutant retinal precursor cells.

Ectopic retinal ganglion cells and photoreceptors in *moe* mutants have normal birthdates

Normally, cells in the innermost part of the retina, retinal ganglion cells, have early birthdays and cells in the outer part of the retina, including photoreceptors, have late birthdays (L. W. Nawrocki, PhD thesis, University of Oregon, 1985). We used birthdating analysis to determine whether the ectopic retinal ganglion cells adjacent to the RPE are born early, like wild-type retinal ganglion cells, and whether ectopic photoreceptors in the inner part of the retina in *moe* mutants are born later, like wild-type photoreceptors.

In wild-type embryos, retinal ganglion cell neurogenesis is complete in the central retina by 42 h (L. W. Nawrocki, PhD thesis, University of Oregon, 1985). To determine whether ectopic retinal ganglion cells in *moe* mutants were born before 42 h, we treated embryos with BrdU from 42-60 h, and then double-labeled sections with the ganglion cell marker, Zn5, and anti-BrdU. In wild-type retinas, retinal ganglion cells in the central retina were BrdU negative (Fig. 5A). In *moe* mutant retinas, retinal ganglion cells, both in the inner retina and adjacent to the RPE, were BrdU negative (Fig. 5B).

In wild-type retinas, photoreceptor neurogenesis begins after about 48 h (L. W. Nawrocki, PhD thesis, University of Oregon, 1985). To determine whether photoreceptors in the inner retina in *moe* mutant embryos are born during the normal period of neurogenesis, we treated embryos with BrdU from 50-74 h and then at 4 d we triple-labeled sections with the photoreceptor markers, Zpr1 (Larison and Bremiller, 1990) and Zpr3, and anti-BrdU. In wild-type retinas, many photoreceptors were BrdU positive (Fig. 5C). In *moe* mutant retinas, many photoreceptors were BrdU positive, including those in the inner retina (Fig. 5D). Our birthdating analysis suggests that although cells are in ectopic positions in *moe* mutant embryos, their birthdates are appropriate for their particular cell types.

The *moe* mutation acts cell nonautonomously in dividing and postmitotic retinal cells

To determine whether retinal cells autonomously require wild-type *moe* function to divide in the proper location, we transplanted labeled wild-type cells into unlabeled *moe* mutant hosts at the blastula stage and transplanted labeled *moe* mutant cells into unlabeled wild-type hosts. We then examined the positions of mitotic transplanted cells in the host retinas. We found that many wild-type donor cells in *moe* mutant hosts divided in ectopic positions (Fig. 6A, arrows). In contrast, *moe* mutant donor cells in wild-type hosts divided in the normal position (Fig. 6B, arrows).

We quantified the proportions of ectopically dividing donor cells and compared them to the values from age-matched controls. At 36 h (Fig. 6C) and 48 h (data not shown), wild-type cells transplanted into *moe* mutant hosts behaved phenotypically like *moe* mutant cells, and nearly all *moe* mutant cells transplanted into wild-type hosts behaved phenotypically like wild-type cells. These results suggest that the *moe* mutation acts cell nonautonomously in dividing retinal cells, and that normal *moe* gene function is required in some other cell type.

We also tested whether *moe* gene function acts cell

nonautomously with regard to cell position of differentiated cells by examining the positions of wild-type or *moe* mutant donor photoreceptor cells in *moe* mutant or wild-type host retinas. We identified a subset of photoreceptors using Zpr1 and Zpr3 antibodies. Antibody labeled, wild-type-derived photoreceptors in *moe* mutant host retinas were in ectopic locations, similar to *moe* mutant photoreceptor cells (Fig. 6D, arrows). Isolated single antibody-labeled *moe* mutant cells (Fig. 6E, arrow) or antibody-labeled *moe* mutant cells in small donor groups (Fig. 6E, double arrows) in wild-type host retinas adopted the correct position in the photoreceptor layer adjacent to the RPE. The elongated morphology of isolated single *moe* mutant photoreceptors in wild-type hosts was normal (Fig. 6E, arrow); however, we often observed that when larger numbers of *moe* mutant retinal cells were present, the morphology of photoreceptor cells was abnormal (Fig. 6E, double arrows). In cases where very large numbers of *moe* mutant cells were transplanted into wild-type host retinas, ectopic photoreceptors were observed in the retinal ganglion cell layer (data not shown). These results suggest that the *moe* mutation also acts cell nonautonomously in postmitotic cells with regard to cell position.

Transplanted wild-type RPE rescues the cell division defect of *moe* mutant retinal cells

Our observation that normal *moe* function is not required within dividing retinal cells suggested the possibility that normal *moe* function is required in the RPE. To test this hypothesis, we transplanted labeled wild-type blastomeres into *moe* mutant host embryos of the same stage. We then examined the positions of dividing retinal cells adjacent to wild-type derived RPE at 42 h. We found that wild-type RPE could restore the normal positions of dividing retinal cells in *moe* mutant embryos (Fig. 7A, arrow). We quantified the results of transplanting wild-type RPE into *moe* mutant eyes and found that only about 13% of retinal cells divided ectopically (seven ectopic divisions in a total of 55 divisions analyzed) when adjacent to wild-type RPE, 2.5% of cells divided ectopically in wild-type siblings, whereas 61.4% of cells divided ectopically in *moe* mutant siblings (Fig. 7B). These results suggest that *moe* function is required in the RPE to localize dividing retinal cells to the RPE surface.

DISCUSSION

We have described our analysis of mutations of the *mosaic eyes* gene that cause RPE abnormalities, retinal abnormalities that include the loss of localization of dividing cells to the RPE surface, the loss of lamination, reduced brain ventricles, heart and/or circulation abnormalities and dorsal curvature of the tail. We have isolated two *moe* alleles, *moe^{b476}* (γ-ray induced) and *moe^{b781}* (ENU induced) that have indistinguishable phenotypes suggesting that a single gene is mutated, although we cannot rule out the possibility that both mutations affect more than one gene.

We found that retinal cell types differentiate even though their positions are abnormal in *moe* mutants (Fig. 2). This result is similar to that observed with many brain mutants (for review, see Rice and Curran, 1999), suggesting that in both the brain and retina, the process of differentiation is largely independent from the positioning of differentiated cells. We often observed a reduction in amacrine cells and Müller glia in *moe* mutant retinas. This could be due to the increased cell death we observed at late stages of development (48 h and older; data not shown) or, alternatively, fewer retinal epithelial cells may adopt amacrine cell and Müller glial cell fates in *moe* mutant retinas.

The positions of retinal ganglion cells that are the first cells to become postmitotic (L. W. Nawrocki, PhD thesis, University of Oregon, 1985; Hu and Easter, 1999) were least affected in *moe* mutants and many were in the normal position. The positions of photoreceptors that are among the last cells to become postmitotic (L. W. Nawrocki, PhD thesis, University of Oregon, 1985) are most affected in *moe* mutants; sometimes they are scattered throughout the thickness of the retina, and often they form layers in the wrong position. The abnormal positions of differentiated cells may be a consequence of retinal precursor cells dividing in the wrong place, and photoreceptors may be more affected than retinal ganglion cells because more precursor cells divide ectopically when photoreceptors form than earlier when retinal ganglion cells form (Fig. 3; L. W. Nawrocki, PhD thesis, University of Oregon, 1985). Although many retinal ganglion cells and photoreceptors occupy abnormal positions in *moe* mutants they become postmitotic at times appropriate for their particular cell type (Fig. 5).

At least some retinal epithelial cells have normal interphase morphologies in *moe* mutants (Fig. 4). Except during mitosis, retinal epithelial cells normally extend processes to the vitreal (basal) and RPE (apical) surfaces. When cells enter mitosis at the apical surface, they retract their basal process (Sidman, 1961). Our analysis of the morphologies of retinal epithelial cells suggests that precursor cells are capable of extending processes to the apical and basal surfaces in *moe* mutants (Fig. 4). We observed that large numbers of retinal cells continue to divide throughout the retina in older *moe* mutants (Fig. 2H), whereas division is confined to a small number of cells in the marginal zone in wild-type retinas (Fig. 2G), suggesting the possibility that in *moe* mutants, mitogenic signals fail to be downregulated or that inhibitors of proliferation fail to be upregulated.

Some of the *moe* mutant phenotypes are distinct from those of the previously described *oko meduzy* mutation (Malicki and Driever, 1999). Approximately half as many cells divide ectopically at 30 h in *moe* mutant retinas compared to *ome* mutant retinas (Malicki and Driever, 1999). Moreover, many *ome* mutant retinal cells lose continuity with the RPE (apical) surface (Malicki and Driever, 1999), whereas many *moe* mutant retinal epithelial cells extend apparently normal apical and basal processes. It will be interesting to determine whether *oko meduzy* and *mosaic eyes* act in the same genetic pathway.

Normal *moe* function is required in RPE cells

We performed genetic mosaic analysis to determine whether wild-type *moe* function is required within dividing retinal epithelial cells to apically localize cell divisions. We found that wild-type retinal cells transplanted into *moe* mutant hosts divided ectopically like mutant cells and that most *moe* mutant retinal cells transplanted into wild-type hosts divided in the normal apical position (Fig. 6). This analysis suggests that *moe* function is not required within dividing retinal cells.

Fig. 5. Ectopic retinal ganglion cells and photoreceptors in *moe* mutant embryos have normal birthdates. Embryos were treated with BrdU from 42-60 h, and then sections were double-labeled with the ganglion cell marker, Zn5 (red), and anti-BrdU (green). In wild-type retinas, retinal ganglion cells in the central retina are BrdU negative (A). In *moe* mutant retinas, retinal ganglion cells, both in the inner retina and cells near the RPE (arrows) are BrdU negative (B). Embryos were treated with BrdU from 50-74 h and at 4 d sections were triple labeled with the photoreceptor markers, Zpr1 and Zpr3 (red), and anti-BrdU (green). In wild-type retinas, many photoreceptors are BrdU positive (C). In *moe* mutant retinas, many photoreceptors are BrdU positive, including those in the inner part of the retina (D, arrows). Scale bar: 50 μm.
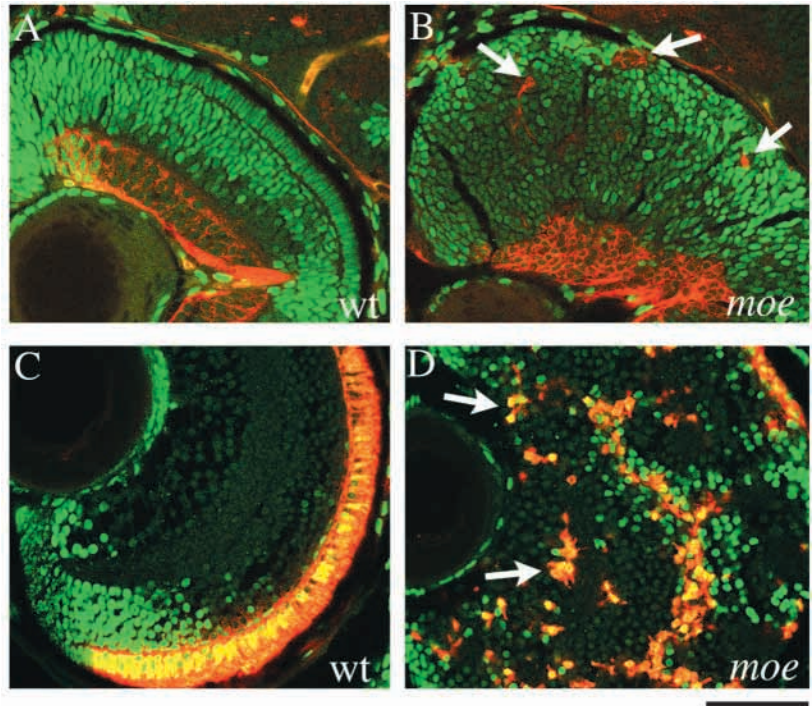
Our further analysis suggests that *moe* function is required in the RPE for the apical localization of cell divisions in the neural retina. We transplanted wild-type RPE into *moe* mutants and examined the positions of dividing cells adjacent to wild-type RPE. Wild-type RPE restored the normal positions of dividing retinal cells in *moe* mutants, consistent with the hypothesis that normal *moe* function is required in the RPE (Fig. 7).

We observed no defects in the positions of dividing cells or neurons in the brain (Fig. 3) and spinal cord in *moe* mutants, suggesting that the normal function of *moe* is required specifically for the positioning of dividing cells and neurons in the retina. None of the reported mouse mutations that affect the positions of neurons or lamination in the brain (for review, see Rice and Curran, 1999) affect lamination in the retina, further supporting the notion that the processes of layer formation in
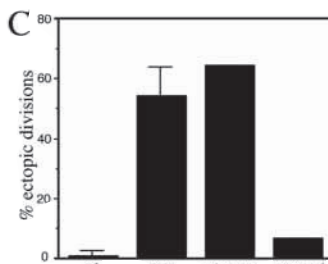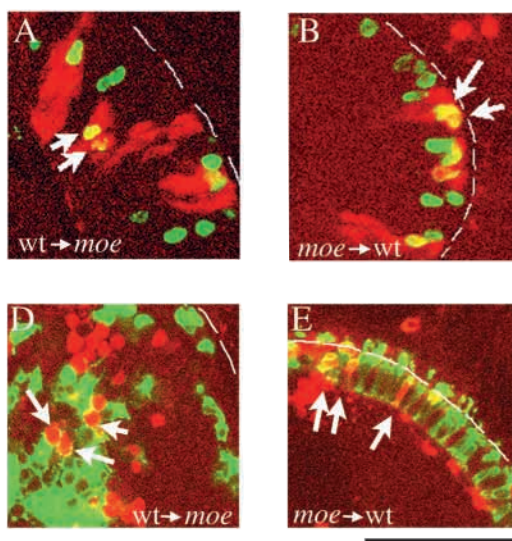

Fig. 6. Genetic mosaic analysis demonstrates that *moe* acts cell nonautonomously in dividing and postmitotic retinal cells. We tested whether the *moe* mutation acts cell autonomously in dividing retinal cells and photoreceptors by transplanting rhodamine-labeled blastomeres into unlabeled host embryos. To examine the positions of dividing cells we labeled sections with anti-H3 antibodies to show dividing cells. (A,B) Confocal images of sections showing donor-derived cells (red) and anti-H3 labeled cells (green), double-labeled cells are yellow. (A) Many wild-type cells transplanted into *moe* mutant hosts divided ectopically (arrows). (B) *moe* mutant cells transplanted into wild-type hosts divided at the RPE surface (arrows). We calculated the proportions (number of ectopic divisions divided by total number of divisions) of ectopically dividing donor cells in genetic mosaics at 36 h (C). We scored anti-H3-labeled cells as ectopic in wild-type and *moe* mutant retinas if they were more then one cell diameter away from the RPE. For comparisons, age-matched controls (wt, *moe*; from Fig. 3C) are included. At 36 h, 32/49 labeled wild-type cells divided ectopically in *moe* mutant embryos (wt→*moe*; five embryos), and 3/42 labeled *moe* mutant cells divided ectopically in wild-type embryos (*moe*→wt; five embryos). To examine the positions of photoreceptor cells we labeled sections with Zpr1 and Zpr3 antibodies at 4 d. (D,E) Confocal images of sections showing donor-derived cells (red) and Zpr3-labeled cells (green). (D) Many wild-type derived photoreceptor cells in a *moe* mutant host retina are in ectopic locations (arrows). (E) In cases where isolated single cells or small numbers of *moe* mutant photoreceptors are present in wild-type host retinas they are in the photoreceptor layer (arrows). Single cells have normal elongated morphologies (single arrow), but larger groups of *moe* mutant cells can have abnormal morphologies (double arrows). We examined three embryos where wild-type derived cells generated photoreceptors in *moe* mutant hosts and three embryos where *moe* mutant-derived cells generated photoreceptors in wild-type hosts. The RPE surface is outlined (A,B). Scale bar: A-D, 50 μm.

Fig. 7. Transplanted wild-type RPE restores the normal position of dividing cells in *moe* mutant retinas. We transplanted rhodamine-labeled wild-type blastomeres into unlabeled *moe* mutant host embryos. The positions of dividing retinal cells adjacent to wild-type donor derived RPE cells (yellow) were determined by labeling sections with anti-H3 antibodies (green) at 42 h. (A) Example of *moe* mutant retinal cells dividing in the normal position when adjacent to wild-type RPE cells (arrow). The lens is outlined. (B) We calculated the proportions (number of ectopic divisions divided by total number of divisions) of ectopically dividing cells adjacent to wild-type donor derived RPE cells. Retinas from three hosts were analyzed and we found seven cells that divided ectopically in a total of 55 dividing cells (~13%) that were adjacent to wild-type donor-derived RPE (16 cases). For comparison, we calculated the average proportions of ectopically dividing retinal cells in three wild-type and three *moe* mutant siblings of the host embryos. At 42 h, the mitotic zone (containing H3$^+$ cells) is two cell diameters wide in wild-type embryos; therefore, we scored anti-H3 labeled cells as ectopic in wild-type and *moe* mutant retinas if they were more than two cell diameters away from the RPE. Error bars represent s.e.m. Scale bar: 50 μm.
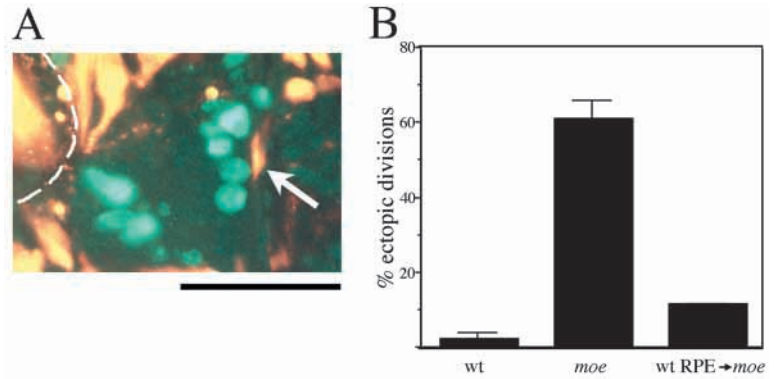
the brain and retina require the functions of different genes. A difference between the developing retina and brain is that the apical (ventricular) surface of the retina is adjacent to the RPE, whereas there is no cell type analogous to the RPE adjacent to the ventricular surface of the brain. In vitro studies of reaggregate retinal cultures have shown that retinal cells fail to form proper layers when grown in the absence of RPE cells, but if RPE cells are included in the reaggregates (Vollmer et al., 1984; Layer and Willbold, 1989) or reaggregates are cultured above a monolayer of RPE cells (Rothermel et al., 1997) then the reaggregates form layers in the same order as found in vivo. These studies suggest that the RPE plays an important role in generating the correct polarity of retinal layers. Further support for the hypothesis that the RPE is required for normal retinal layer formation comes from in vivo studies. Mouse RPE cells were genetically ablated using a diphtheria toxin transgene under the control of the tyrosinase-related protein 1 promoter (Raymond and Jackson, 1995). When RPE cells were ablated very early in development, the mice were largely anophthalmic; however, if RPE cells were ablated later, the eye developed but the organization of the retina adjacent to those regions where the RPE was ablated was severely disrupted (Raymond and Jackson, 1995). Layer and Willbold (Layer and Willbold, 1989) have suggested that the RPE is required to generate the correct sequence of retinal layers. It may, thus, be significant that we observed cryptic or partial photoreceptor layers in the innermost part of *moe* mutant retinas, the region normally occupied by retinal ganglion cells, a position opposite to where the photoreceptor layer normally forms (Fig. 2). This result may suggest that the polarity of the retina is reversed, at least partially, in the absence of *moe* function in RPE cells.

A common feature of retinal reaggregate cultures grown in the absence of RPE is the formation of clusters or rosettes of cells, rather than layers (for a review, see Layer and Willbold, 1993). Rosettes were also observed in retinas in which RPE cells were ablated in vivo (Raymond and Jackson, 1995). We did not observe rosettes in *moe* mutant retinas. One interpretation of this difference is that the *moe* mutation does not produce the same cellular environment that encourages rosette formation in vivo following RPE ablation or in reaggregate cultures.
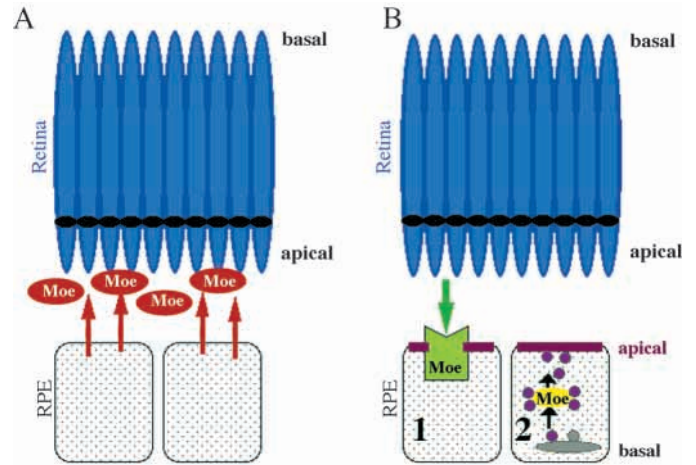
Fig. 8. Models of the normal function of Moe protein in organizing the positions of retinal cells. (A) Moe is a RPE-derived signal, or regulates the production or release of such a signal, that instructs retinal cells to divide apically. (B) Moe is involved in generating the correct apical-basal polarity in the RPE and correct RPE polarity is necessary for proper RPE signaling to the retina. (1) Moe could be a receptor for signals released by the retina that instruct the correct polarity of the RPE or (2) Moe could be involved in the process of establishing apical polarity, for example, by targeting vesicles to the apical membrane.

Our analysis suggests that the *moe* mutation identifies a gene required in the RPE to mediate its organizing effects on the neural retina. We propose that in *moe* mutants, RPE cells fail to signal properly to the neural retina to establish the correct polarity of the retinal epithelium, so that retinal cells no longer distinguish which direction is apical and which is basal.

moe functions to organize retinal cell position

We propose two alternative models of wild-type Moe protein function in signaling from the RPE to the neural retina (Fig. 8). In Model A, Moe is the signal, or functions in the production or release of such a signal, generated by the RPE that regulates the positioning of dividing and differentiated cells in the retina (Fig. 8A). Perhaps this signal provides an apical polarity cue to the retina.

In Model B, Moe is required for the correct polarity of the RPE and RPE polarity is necessary for proper signaling to the adjacent neural retina. Although the RPE shares some polarity characteristics with other epithelia, such as sites of viral budding (Bok et al., 1992), it also has polarity characteristics that are reversed relative to those of other epithelia. For example, the RPE targets several proteins to the apical surface that are targeted basolaterally in other epithelia, including the Na/K-ATPase (Bok, 1982) and the cytoskeletal proteins, fodrin and ankyrin (Gundersen et al., 1991). Although the Na/K-ATPase is apical in the RPE in vivo, it is both apical and basalolateral in isolated RPE cells grown in culture (Rizzolo, 1990). If retinal epithelium is included in cultures of RPE, however, aspects of normal RPE polarity are observed (Rizzolo, 1999), suggesting that the retina provides polarizing cues to the RPE. The normal function of Moe protein could be as a receptor, or component downstream of such a receptor, for a retinal-derived signal that polarizes the RPE (Fig. 8B, cell 1). Alternatively, Moe could be a component of the machinery that generates RPE polarity; perhaps Moe is involved in targeting vesicles to the apical membrane (Fig. 8B, cell 2). It may be important to add that the polarity of the RPE has been shown to be developmentally regulated (Rizzolo and Heiges, 1991), and we observed an increasing requirement for *moe* function during retinal development (Fig. 3D).

Like the RPE, the choroid plexus is among the few epithelia that exhibit aspects of reversed polarity, including the apical localization of Na/K-ATPase, fodrin and ankyrin (Alper et al., 1994). The choroid plexus secretes the cerebral spinal fluid that fills the ventricular space in the brain. *moe* mutants fail to inflate the brain ventricles properly, suggesting that the secretion of cerebral spinal fluid by the choroid plexus may be abnormal.

Our analysis of the *moe* mutation provides the first genetic evidence that RPE-derived factors are required for proper retinal organization. Several other mutations in zebrafish have been identified that affect the RPE and the organization of retinal cells (Malicki et al., 1996; Malicki and Driever, 1999); the cell types in which the normal functions of these genes are required, however, have not been identified. Given the apparent similarities of these mutant phenotypes, we suggest the possibility that these mutations, as a class, reveal the reciprocal signaling pathway between the RPE and the neural retina, where each tissue relies on its neighbor to establish polarity and proper patterning.

REFERENCES

Aroca, P., Garcia-Borron, J. C., Solano, F., Lozano, J. A. (1990). Regulation of mammalian melanogenesis. I. Partial purification and characterization of a dopachrome converting factor: Dopachrome tautomerase. *Biochim. Biophys. Acta* **1035**, 266-275.

Babin, P. J., Thisse, C., Durliat, M., Andre, M., Akimenko, M-A. and Thisse, B. (1997). Both apolipoprotein E and A-1 genes are present in a nonmammalian vertebrate and are highly expressed during embryonic development. *Proc. Natl. Acad. Sci. USA* **94**, 8622-8627.

Bok, D. (1982). Audioradiographic studies on the polarity of plasma membrane receptors in retinal pigment epithelial cells. In *The Structure of the Eye* (ed. J.G. Hollyfield), pp. 247-256. New York: Elsevier North Holland.

Bok, D., O'Day, W. and Rodriguez-Boulan, E. (1992). Polarized budding of vesicular stomatitis and influenza virus from cultured human and bovine retinal pigment epithelium. *Exp. Eye Res.* **55**, 853-860.

De Leeuw, A. M., Gaur, V. P., Saari, J. C., and Milam, A. H. (1990). Immunolocalization of cellular retinol-, retinaldehyde-, and retinoic acid-binding proteins in rat retina during pre- and postnatal development. *J. Neurocyt.* **19**, 253-264.

Fashena, D. and Westerfield, M. (1999). Secondary motoneuron axons localize DM-GRASP on their fasciculated segments. *J. Comp. Neurol.* **406**, 415-424.

Gundersen, D., Orlowski, J. and Rodriguez-Boulan, E. (1991). Apical polarity of Na,K-ATPase in retinal pigment epithelium is linked to a reversal of the ankyrin-fodrin submembrane cytoskeleton. *J. Cell Biol.* **112**, 863-872.

Hendzel, M. J., Wei, Y., Mancini, M. A., Van Hooser, A., Ranalli, T., Brinkley, B. R., Bazett-Jones, D. P., and Allis, C. D. (1997). Mitosis-specific phosphorylation of histone H3 initiates primarily within pericentromeric heterochromatin during G2 and spreads in an ordered fashion coincident with the mitotic chromosome condensation. *Chromosoma* **106**, 348-360.

Ho, R. K. and Kane, D. A. (1990). Cell-autonomous action of zebrafish *spt-1* mutation in specific mesodermal precursors. *Nature* **348**, 728-730.

Hu, M., and Easter, S. S. (1999). Retinal neurogenesis: the formation of the initial central patch of postmitotic cells. *Dev. Biol.* **207**, 309-321.

Johnson, S. L., Gates, M. A., Johnson, M., Talbot, W. S., Horne, S., Baik, K., Rude, S., Wong, J. R., and Postlewait, J. H. (1996). Centromere-linkage analysis and consolidation of the zebrafish genetic map. *Genetics* **142**, 1277-1288.

Larison, K. D. and Bremiller, R. (1990). Early onset of phenotype and cell patterning in the embryonic zebrafish retina. *Development* **109**, 567-576.

Layer, P. G. and Willbold, E. (1993). Histogenesis of the avian retina in reaggregation culture: From dissociated cells to laminar neuronal networks. *Int. Rev. Cytol.* **146**, 1-46.

Layer, P. G. and Willbold, E. (1989). Embryonic chicken retinal cells can regenerate all cell layers in vitro, but ciliary pigmented cells induce their correct polarity. *Cell Tissue Res.* **258**, 233-242.

Linser, P.J., Smith, K. and Angelides, K. (1985). A comparative analysis of glial and neuronal markers in the retina of fish: variable character of horizontal cells. *J. Comp. Neurol.* **237**, 264-272.

Malicki, J., Neuhauss, S. C., Schier, A. F., Solnica-Krezel, L., Stemple, D. L., Stainier, D. Y. R., Abdelihah, S., Zwartkruis, F., Rangini, Z., and Driever, W. (1996). Mutations affecting development of the zebrafish retina. *Development* **123**, 263-273.

Malicki, J. and Driever, M. (1999). oko meduzy mutations affect neuronal patterning in the zebrafish retina and reveal cell-cell interactions of the retinal neuroepithelial sheet. *Development* **126**, 1235-1246.

Marusich, M. F., Fruneaux, H. M., Henion, P. D., and Weston, J. A. (1993). Hu neuronal proteins are expressed in proliferating neurogenic cells. *J. Neurobio.* **25**, 143-155.

Pawelek, J., Korner, A., Bergstrom, A., Bologna, J. (1980). New regulators melanin biosynthesis and the autodestruction of melanoma cells. *Nature* **286**, 617-619.

Raymond, S. M. and Jackson, I. J. (1995). The retinal pigmented epithelium is required for development and maintenance of the mouse neural retina. *Curr. Biol.* **5**, 1286-1295.

Rice, D. S. and Curran, T. (1999). Mutant mice with scrambled brains: understanding the signaling pathways that control cell positioning in the CNS. *Genes Dev*. **13**, 2758-2773.

Riley, B. B. and Grunwald, D. J. (1995). Efficient induction of point mutations allowing recovery of specific locus mutations in zebrafish. *Proc. Natl. Acad Sci. USA* **92**, 5997-6001.

Rizzolo, L. J. (1990). The distribution of Na,K-ATPase in the retinal pigmented epithelium from chicken embryo is polarized in vivo but not in primary cell culture. *Exp. Eye Res.* **51**, 435-446.

Rizzolo, L. J. and Heiges, M. (1991). The polarity of the retinal pigment epithelium is developmentally regulated. *Exp. Eye Res*. **53**, 549-553.

Robinson, J. Schmitt, E. A. and Dowling, J. E. (1995). Temporal and spatial patterns of opsin gene expression in zebrafish (*Danio rerio*). *Vis. Neurosci.* **12**, 895-906.

Rothermel, A., Willbold, E. Degrip, W. J., and Layer, P. G. (1997). Pigmented epithelium induces complete reconstitution from dispersed embryonic chick retinae in reaggregation culture. *Proc. R Soc. London B Biol. Sci*. **264**, 1293-1303.

Sandell, J., Martin, S. and Heinrich, G. (1994). The development of GABA immunoreactivity in the retina of the zebrafish. *J. Comp. Neurol.* **345**, 596-601.

Sidman, R. L. (1961). Histogenesis of mouse retina studied with thymidine-H3. In *Structure of the Eye* (ed. G.K. Smeiser), pp. 487-506. New York: Academic Press.

Steel, K. P., Davidson, D. R., and Jackson, I. J. (1992). TRP-2/DT, a new early melanoblast marker, shows that Steel growth factor (c-kit ligand) is a survival factor. *Development* **115**, 1111-1119.

Streisinger, G., Walker, C., Dower, N., Knauber, D., and Singer, F. (1981). Production of clones of homozygous diploid zebrafish (*Brachydanio rerio*). *Nature* **291**, 393-396.

Tsukamoto, K., Jackson, I. J., Urabe, K., Montegue, P. M., and Hearing, V. J. (1992). A second tyrosinase-related protein, TRP-2, is a melanogenic enzyme termed DOPAchrome tautomerase. *EMBO J*. **11**, 519-526.

Trevarrow, B., Marks, D. L. and Kimmel, C. B. (1990). Organization of hindbrain segments in the zebrafish embryo. *Neuron* **4**, 669-679.

Vollmer, G., Layer, P. G. and Gierer, A. (1984). Reaggregation of embryonic chick retinal cells: pigment epithelial cells induce a high order of stratification. *Neurosci Lett.* **48**, 191-196.

Walker, C. (1999). Haploid screens and gamma-ray mutagenesis. In *The Zebrafish: Genetics and Genomics.* (eds. H. W. Detrich, M. Westerfield and L. I. Zon), Vol. 60, pp. 44-70. Academic Press.